On the Role of Overlap between the Discrete state and Pseudo-continuum States in Stabilization Calculations of Metastable States

Stephen R. Slimak[1], Kenneth D. Jordan[1], and Michael F. Falcetta[2]*

[1] Department of Chemistry, University of Pittsburgh, Pittsburgh, PA 15260, United States

[2] Department of Chemistry, Grove City College, Grove City, Pennsylvania 16127 United States

Email: jordan@pitt.edu

Abstract: In a diabatic picture metastable states subject to decay by electron detachment can be viewed as arising from the coupling between a discrete state and a continuum. In treating such states with bound-state quantum chemical methods, the continuum is discretized. In this study, we elucidate the role of overlap in this interaction in the application of the stabilization method to temporary anion states. This is accomplished by use of a minimalist stabilization calculation on the lowest energy $\ell = 2$ (D) resonance of the finite spherical well potential using two basis functions, one describing the diabatic discrete state and the other a diabatic discretized continuum state. We show that even such a simple treatment predicts a complex resonance energy in good agreement with the exact result. If the energy of the discrete state is assumed to be constant, which is tantamount to orthogonalizing the discretized continuum state to the discrete state, it is demonstrated that the square of the off-diagonal coupling has a maximum close to the crossing point of the orthogonalized diabatic curves and that the curvature in the coupling is responsible for the complex stationary point associated with the resonance. Moreover, this curvature is a consequence of the overlap between the two diabatic states.

INTRODUCTION

Metastable states that are subject to electron detachment play a role in a wide range of chemical processes. Examples include temporary anions, electronically excited states above the first ionization potential, and atoms and molecules in electric fields. In this article, we focus on temporary anions, which are subject to electron detachment because they lie energetically above the electronic ground state of the neutral atom or molecule. There are different classes of temporary anions, distinguished by the electron trapping mechanism.[1] Of particular interest are temporary anions that result from electron capture into a low-lying empty valence orbital, with the electron trapping being due to an angular momentum barrier. Such anions appear as shape resonances in various low energy electron scattering cross sections[1-3] and are known to play important roles in a wide range of chemical processes.[4-7]

When standard electronic structure approaches are applied to temporary anions, they are subject to variational collapse, i.e., as the basis set is more extended spatially the wavefunction collapses onto that of the neutral species plus a "free" electron in a discretized continuum (DC) orbital. A variety of methods have been developed to address this issue. These include complex coordinate rotation,[8] the complex absorbing potential (CAP) method,[9] modified potential methods combined with analytic continuation,[10] and the stabilization method.[11] All of these approaches characterize a resonance by a complex energy.[12]

$$E_{res} = E_r - i\Gamma/2, \qquad (1)$$

where E_r and Γ denote the resonance position and half-width respectively in atomic units. The complex energy is consistent with a state that decays exponentially in time.

The present article focuses on the stabilization method which involves calculating the energy levels of the excess electron system as a function of a parameter that controls the extent of the basis set, the size of a constraining box, or the strength of a perturbing potential term in the Hamiltonian. We limit ourselves here to the first approach as used with Gaussian basis functions, in which case the scaling is accomplished by multiplying the exponents of a set of diffuse functions by a scale parameter, denoted here by z.

To set the stage for the present analysis, we show in Figure 1 a stabilization graph for the widely studied Π_g temporary anion of N_2.[1,13-16] This stabilization graph was generated using the equation-of-motion Møller-Plesset (EOM-MP2) method[17,18] with the exponents of four diffuse p functions on each N atom being scaled as described in Ref. 15. The stabilization graph displays two avoided crossings that can be viewed as arising from the interactions between a diabatic discrete state, the energy of which is independent or only weakly dependent on the scale parameter, and a set of diabatic discretized continuum levels whose energies depend strongly on the scale parameter. Various methods can be used to extract the resonance energy and width from a stabilization graph,[19-22] the most common of which is to analytically continue the energies into the complex plane and to find complex stationary points z^* for which $dE/dz = 0$. These appear as complex conjugate pairs. Substitution of these z^* values back into the expression for the energy gives complex energies, which again occur as complex

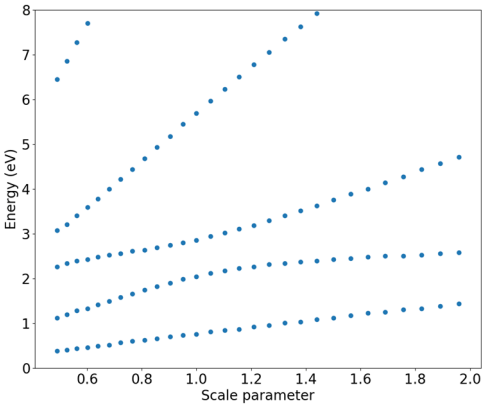

Figure 1. Stabilization graph for the Π_g anion of N_2 at its equilibrium geometry calculated using the EOM-MP2 method and multiplying the exponents of four diffuse p functions on each atom by the scale factor z.

conjugate pairs, with the solution with the negative imaginary part being that associated with the resonance.[19,20] In general, the analytic continuation is done using generalized Pade´ approximants (GPAs)[23] or continued fractions. Alternatively, in the case of a reasonably well isolated avoided crossing, one can choose physically motivated functional forms for the two diabatic states, one describing the discrete state and the other a DC level, as well as for their off-diagonal coupling.[22,24]

In a two-level characterization of an avoided crossing in a stabilization graph, it is useful to associate wave functions ψ_1 and ψ_2 with the discrete state and the DC level, respectively, and with the corresponding energies denoted by H_{11} and H_{22}. In the analysis that we presented in Ref. 24, we chose H_{11} to be independent of the scale parameter and further orthogonalized ψ_2 to ψ_1, giving $\tilde{\psi}_2$. With these assumptions, a two-level treatment allows one to extract the functional form of $\tilde{H}_{12}{}^2$ from the stabilization graph. (The tilde on a matrix element denotes that it includes the effects of orthogonalization of the DC level to the discrete level.) Significantly, this result did not require any assumption about the functional form of $\tilde{H}_{22}$. For the case of the Π_g anion of N_2, $\tilde{H}_{12}{}^2$ deduced from a two-level treatment of the avoided crossing near $z = 1.0$ in the stabilization graph shown in Figure 1 was found to be peaked near the crossing point of the orthogonalized diabatic curves. This result led us to introduce a 2x2 model Hamiltonian for extracting complex resonance energies from a stabilization graph. In addition to the assumption that H_{11} = constant, this model further assumed that the energy of the orthogonalized DC level, $\tilde{H}_{22}$, varies linearly with z and that in the region of the avoided crossing the square of the coupling, $\tilde{H}_{12}{}^2$ is well described by an expression with terms up through quadratic in z. The width as calculated in this model was shown to be proportional to the square root of the absolute

value of the curvature in $\widetilde{H}_{12}{}^2$. In Ref. 24 we conjectured that the curvature in $\widetilde{H}_{12}{}^2$ is a result of the overlap between ψ_2 and ψ_1.

The main objective of the present study is to elucidate the role of overlap in establishing the resonance parameters as deduced from the stabilization method. To this end we consider the lowest energy resonance with angular momentum ℓ=2 (and hereafter referred to as *D*) of a finite spherical well potential. For this problem we perform stabilization calculations with a basis set consisting of a discrete state and a single DC level. While such a treatment is not expected to give a quantitatively accurate resonance energy, it allows for a detailed analysis of the effect of overlap on the off-diagonal coupling and on the resonance parameters. In addition, complex stationary points can be determined for this problem without fitting data points from the stabilization graph to a GPA or other functional form, which allows us to also determine the flexibility required in a GPA to accurately locate the stationary points. These results help in understanding the successes of the stabilization method in describing temporary anions and other metastable states.

COMPUTATIONAL DETAILS

Model Potential and Exact *S*-matrix Results. In order to explore, in detail, the role of overlap between the wave functions of the discrete state and a DC level in determining the location of the relevant stationary point and the associated resonance parameters, we consider the lowest energy *D* resonance of the finite spherical well model with

$$V = -V_0, \text{ for } r < R$$

$$= 0, \text{ for } r \geq R. \qquad (2)$$

This model allows for exact determination of the complex resonance energy (via the associated *S*-matrix[25]), and when used in the context of the stabilization method gives analytical expressions for the overlap and Hamiltonian matrix elements. Due to the spherical symmetry, the resonances resulting from this potential can be associated with the angular momentum ℓ, with the $0.5\ell(\ell+1)/r^2$ angular momentum term (expressed in atomic units) being responsible for the trapping of an electron in low-energy resonances for $\ell \neq 0$. We focus on the $\ell = 2$ case, as it is relevant for the lowest energy temporary anions of N_2 and ethylene, as well as for the *D* shape resonance resulting from electron capture into the 3*d* orbital of the Ca atom.[26] However, the main conclusions of our analysis are equally valid for systems for which the dominant partial wave has other non-zero values of ℓ. We choose $V_0 = 15.51$ eV (0.57 hartree) and $R = 3.8$ bohr, for which the resonance energy is 1.812 - 0.356i eV, as determined from the pole of the *S*-matrix using the exact phase shift. This width is consistent with values reported for N_2 at its equilibrium geometry, although the position is about 0.5 eV below that of the resonance of N_2.

Before presenting results from stabilization calculations on this model system, we briefly consider the analytical results obtained using the phase shift which for the *d*-wave component finite spherical well problem is:

$$\delta=\arctan\left(\frac{\sqrt{2E}\,j_2\left(R\sqrt{2(E+V_0)}\right)j_3\left(R\sqrt{2E}\right)-\sqrt{2(E+V_0)}\,j_2\left(R\sqrt{2E}\right)j_3\left(R\sqrt{2(E+V_0)}\right)}{\sqrt{2E}\,j_2\left(R\sqrt{2(E+V_0)}\right)n_3\left(R\sqrt{2E}\right)-\sqrt{2(E+V_0)}\,n_2\left(R\sqrt{2E}\right)j_3\left(R\sqrt{2(E+V_0)}\right)}\right) \qquad (3)$$

where R and V_0 (in atomic units) are the potential parameters and j_ℓ and n_ℓ are, respectively, the spherical Bessel and spherical Neumann functions associated with angular momentum ℓ. This result was obtained using the fact that the exact wave function involve a spherical Bessel function for $r < R$ and as a linear combination of spherical Bessel and Neumann functions $r \geq R$,

and matching the wave functions and their derivatives for the two regions at $r = R$. This result is then used to calculate the S-matrix using

$$S_D = e^{-2i\delta}, \tag{4}$$

where the "D" subscript denotes that we are focusing on d-wave symmetry and to distinguish this from the symbol we use later to denote overlap. The complex resonance energies are then associated with the poles of the S_D which are given by the zeros of

$$\begin{aligned}&\sqrt{2E}\,j_2\left(R\sqrt{2(E+V_0)}\right)\left[j_3\left(R\sqrt{2E}\right)+n_3\left(R\sqrt{2E}\right)i\right]-\\&+\sqrt{2(E+V_0)}\,j_3\left(R\sqrt{2(E+V_0)}\right)\left[j_2\left(R\sqrt{2E}\right)+n_2\left(R\sqrt{2E}\right)i\right]=0\end{aligned} \tag{5}$$

As noted above, for our choice of parameters, the lowest energy D resonance is located at 1.812 – 0.356i eV. There are also very broad, higher energy resonances located energetically above the angular momentum barrier that are not relevant for the purpose of the current study. The contribution to the cross section in atomic units from the ℓ^{th} partial wave is given by

$$\sigma_\ell = 2\pi \frac{(2\ell+1)}{\sqrt{E}} \sin^2(\delta_\ell) \tag{6}$$

Figure 2 displays as a function of E the phase shift and cross section for d-wave scattering for the model potential with the choice of parameters given above. Note that for an "ideal" resonance, for which $\Gamma << E_r$, the phase shift undergoes a jump of π radians as the energy moves through the resonance region. For the model potential parameters employed, Γ is about 40% of E_r in magnitude, and, as a result, the phase shift jump is only about 2.4 radians and the peak in the cross section is about 0.14 eV above E_r, as determined from the pole of the S-matrix. Depending on the choice of parameters defining the potential, the resonance can be tuned from one with a phase shift jump of π to one that is even further removed from ideal than that considered here.

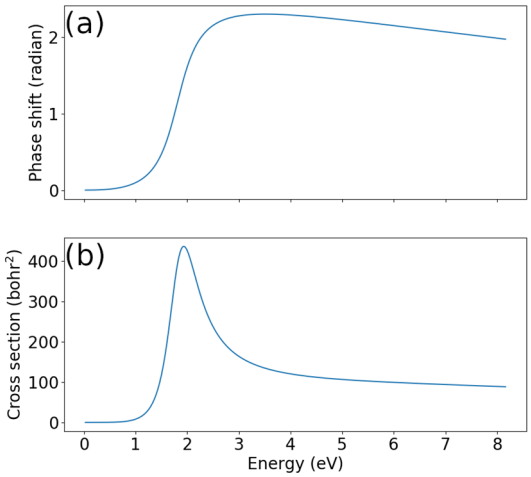

Figure 2. Phase shift (a) and cross section (b) vs. E in the vicinity of the lowest energy D resonance of the finite spherical well problem.

Stabilization Calculations. We now turn to application of the stabilization method to the spherical well problem. Most stabilization calculations on molecules have been carried out using Gaussian type orbitals (GTOs),[14,15,27] and for this reason we use GTOs here, focusing on the d_{xy} component. For stabilization calculations on molecules, it is customary to scale only the diffuse basis functions of the relevant symmetry. In part, this is because the tight functions generally also play a role in describing the occupied orbitals of the neutral molecule. E.g., in stabilization calculations on the π^* anion of N_2, one often scales a set of diffuse p functions centered on each N atom. If one also scaled the tight p functions this would significantly impact the energies of the occupied π_u and σ orbitals of the neutral molecule. Obviously, if one were using a code that

allowed one to scale only basis functions of π_g symmetry, the direct impact on the occupied orbitals would be eliminated but the problem would still be present due to the role of "tight" π_g virtual orbitals in correlating the valence orbitals. Note, that stabilization calculations on the Π_g anion of N_2 could be carried out by scaling a set of diffuse *d* functions located at the bond center, but the basis set would still have "tight" unscaled π_g functions. Although this is not generally stated in papers applying the stabilization method, it is often the case that the unscaled tight functions of the relevant symmetry provide a reasonable estimate of the energy for the discrete state. With this in mind, we have carried out a stabilization calculation on the spherical well problem in which we first generate a basis function that approximates the discrete state. This function is represented in terms of five GTOs with exponents of 0.045, 0.090, 0.180, 0.360, and 0.720. The exponents were chosen so that the discrete state has an energy close to that of E_r. Specifically, the calculation with this basis set locates the discrete state at 1.867 eV, only 0.055 eV above the resonance position as established from the *S*-matrix. The coefficients obtained by minimizing the energy are reported in the Supporting Information. The radial probability distribution function of the discrete state is shown in Figure 3 from which it is seen that a significant portion of the charge is in the barrier region. The stabilization calculations are

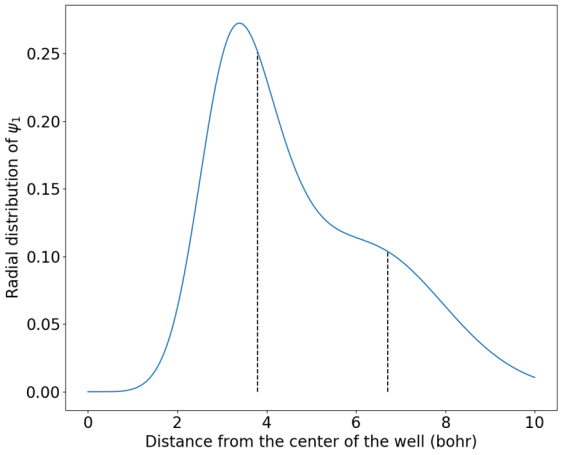

Figure 3. Plot of the radial probability distribution function of the discrete state of the finite spherical well problem with $R = 3.8$ bohr and $V_0 = 0.57$ hartree. The left vertical line indicates the radius of the well and the right vertical line indicates the distance at which the energy of the angular momentum barriers equals that of the discrete state.

then carried out using two basis functions, one corresponding to the discrete state with fixed coefficients and the other being a single primitive GTO with an exponent 0.025 which is multiplied by the scale parameter, z. The analytical expressions for the overlap and kinetic and potential energy integrals are reported in the Supporting Information.

We now return to the issue of locating the stationary points and the resonance energy from the stabilization graph. Although, our two-level treatment of the finite spherical well problem permits determining these quantities directly from analytical expressions for the energy eigenvalues, for stabilization calculations on molecular systems, this is not possible in general. Instead, the usual approach involves fitting the data from the two curves involved in an avoided crossing to an appropriate function of z and using this to determine the complex stationary points. One of the most common approaches for doing this makes use of GPAs which incorporate the branch point structure of an avoided crossing.[23] The quadratic GPA used here is defined as $P(z)E^2 + Q(z)E + R(z) = 0$, where P, Q, and R are polynomials in z. The ijk GPA uses polynomials of order i, j, and k, for P, Q, and R, respectively.

RESULTS AND DISCUSSION

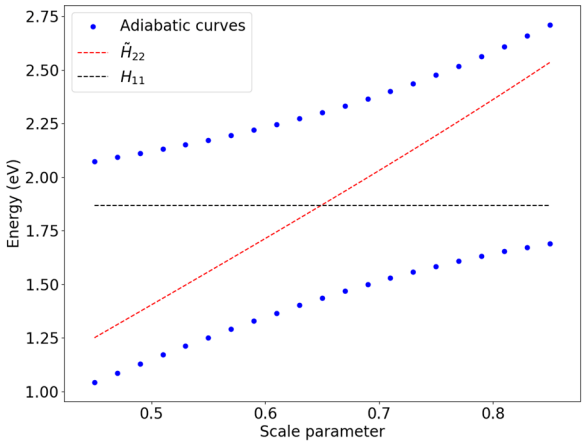

Figure 4. Stabilization graph for the finite spherical well problem using the discrete state depicted in Figure 3 and a single scaled diffuse GTO. The dashed lines indicate the diabatic levels (H_{11} and $\tilde{H}_{22}$) and the dots the adiabatic energy levels.

Stabilization Calculations. Figure 4 displays the stabilization graph for the two basis function treatment of the *D* resonance of the finite spherical well problem. Also included in the figure are the energies of the discrete state and the orthogonalized DC level. There is a clear avoided crossing near $z = 0.65$. As will be seen below, it is essential to account for both the presence of the potential and the orthogonalization of ψ_2 to ψ_1 in determining the crossing point of diabatic curves.

The stationary point, z^*, obtained by solving $dE/dz = 0$ where E is the analytical expression for the energy obtained from the two basis function treatment, is 0.580-0.386i. Interestingly, the real part of z^* is appreciably shifted from the point of closest approach of the two energy levels as well as from the crossing point of H_{11} and $\tilde{H}_{22}$. The associated complex energy is 2.071 – 0.278i eV in reasonable agreement with the exact result of 1.822 – 0.356i eV obtained from the *S*-matrix. The fact that one can obtain reasonable resonance parameters from a stabilization calculation using only two basis functions may be surprising to many readers as applications of the method generally employ basis sets with multiple scaled diffuse functions. However, to get qualitatively accurate results from such simple calculations requires having a reasonable description of the discrete state. For quantitatively accurate results one does need to employ a basis set with more than one scaled diffuse basis function, but for the purpose of examining in

detail the role of overlap on the resonance parameters, this minimalist basis set treatment is very useful.

In general, stabilization calculations on atoms and molecules have multiple sources of error, including those due to basis set truncation and approximations in the treatment of electron correlation as well as those associated with the analytic continuation procedure. Obviously, a one electron model potential treatment is free of electron correlation errors. Also, because we can determine the exact stationary point and resonance energy for the two basis function treatment of the finite spherical well problem, we are able to separate errors due to analytic continuation from those from basis set deficiencies. The results of various GPA fits to data points between $z = 0.45$ and 0.85 are summarized in Table 1. We also report in the Table the branch point with negative imaginary part associated with the avoided crossing. For the two basis function treatment, accurate location of the branch and stationary points and determination of the resonance energy is achieved is achieved by the 345 GPA with 14 parameters, and the 035 GPA with only 10 parameters performs nearly as well. Even the 6-parameter 013 GPA gives an accurate value for the complex resonance energy, but this is likely fortuitous given the fact that the 024 GPA treatment fares less well.

Table 1. Branch points and stationary points and associated energies (eV) from GPA fits to the stabilization graph shown in Figure 4.

Method[a]	Branch point	Stat. point	Energy at stat. point
012 GPA (5)	0.660 – 0.315i	0.660 – 0.613i	1.888 – 0.259i
013 GPA (6)	0.708 – 0.293i	0.564 – 0.372i	2.080 – 0.264i
024 GPA (8)	0.724 – 0.303i	0.639 – 0.397i	2.054 – 0.318i
123 GPA (8)	0.720 – 0.324i	0.661 – 0.474i	2.008 – 0.327i
234 GPA (11)	0.728 – 0.310i	0.643 – 0.412i	2.057 – 0.310i
035 GPA (10)	0.723 – 0.306i	0.589 – 0.422i	2.052 – 0.278i
135 GPA (11)	0.723 – 0.305i	0.603 – 0.393i	2.065 – 0.288i
345 GPA (14)	0.723 – 0.304i	0.583 – 0.350i	2.085 – 0.275i
456 GPA (17)	0.723 – 0.306i	0.580 – 0.386i	2.070 – 0.278i
Exact	0.723 – 0.306i	0.580 – 0.386i	2.068 – 0.278i

[a] The number of parameters in the GPA is indicated in parentheses.

We now turn to the issue of the role of overlap between the discrete state and the DC level in establishing the complex resonance energy. Since only ψ_2 is scaled, the energy of the discrete state, H_{11} is independent of z. The relevant matrix elements are

$$\widetilde{H}_{12} = \frac{H_{12} - SH_{11}}{\sqrt{1-S^2}} \tag{7}$$

and

$$\widetilde{H}_{22} = \frac{H_{22} - 2SH_{12} + S^2 H_{11}}{1-S^2} \tag{8}$$

The resulting adiabatic levels are

$$E_{\pm} = \frac{H_{11} + \widetilde{H}_{22}}{2} \pm \frac{1}{2}\sqrt{\left(H_{11} - \widetilde{H}_{22}\right)^2 + 4\widetilde{H}_{12}^{\,2}} \tag{9}$$

Note that the adiabatic energies, unlike the energies of the diabatic states and their off-diagonal coupling, do not depend on the choice made for the orthogonalization. For a two-level problem one can extract $H_{11} + \widetilde{H}_{22}$ and $\widetilde{H}_{12}^{\,2} - H_{11}\widetilde{H}_{22}$ from the adiabatic energy levels by use of

$$(E_+ + E_-) = H_{11} + \widetilde{H}_{22} \tag{10}$$

$$(E_+ - E_-)^2 = \left(H_{11} + \widetilde{H}_{22}\right)^2 + 4(\widetilde{H}_{12}^{\,2} - H_{11}\widetilde{H}_{22}) \tag{11}$$

With the assumption that H_{11} = constant, one can obtain

$$\widetilde{H}_{12}^{\,2} = H_{11}(E_+ + E_- - H_{11}) - E_+E_- \tag{12}$$

from the stabilization graph with no further assumptions.

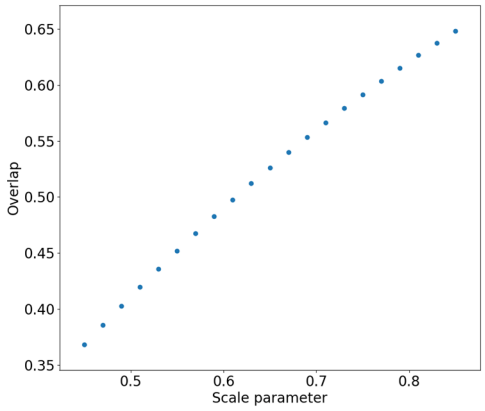

Figure 5. Overlap vs. scale parameter for the two-level treatment of the *D* resonance of the finite spherical well problem.

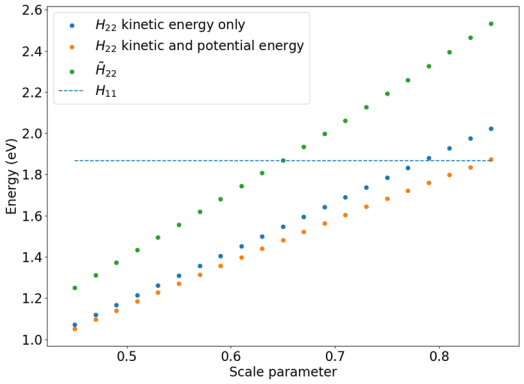

Figure 6. Energy of the DC level in different approximations vs. the scale parameter. H_{22}, unperturbed DC level (blue), H_{22}(KE+PE), including the potential energy (orange), and $\widetilde{H}_{22}$, including both the PE contribution and the effect of orthogonalization (green) for the two-level treatment of the *D* resonance of the finite spherical well problem. The dotted blue horizontal line indicates the energy of the discrete state.

Figures 5 -7 report, respectively, S, H_{22} and $\widetilde{H}_{22}$, H_{12} and $\widetilde{H}_{12}$, determined from the analytical expressions for the relevant matrix elements (reported in the SI) for z values ranging from 0.45 to 0.85, the range that we used use in fitting the adiabatic curves for analytic continuation. From Figure 5 it is seen that the overlap between ψ_1 and ψ_2 is about 0.5 at the crossing point ($z_0 \approx 0.65$) of H_{11} and $\widetilde{H}_{22}$, and moreover, that there is appreciable curvature in S in the vicinity of z_0,

Figure 6 reports the energy of the discrete continuum state unperturbed by the potential, H_{22}, the energy of the discretized continuum state including the influence of the potential H_{22}(KE+PE), and $\widetilde{H}_{22}$ which also includes the effect of orthogonalization of ψ_2 to ψ_1. As seen from this figure, the shift in the energy of the DC level caused by orthogonalization is much greater than that due to the potential energy contribution. It is also seen that for the range of z values displayed, $\widetilde{H}_{22}$ is approximately linear in z, which is somewhat surprising given the significant curvature in S.

This result indicates that there is some cancellation of the various contributions to the curvature in $\widetilde{H}_{22}$.

From Figure 7 it is seen that whereas H_{12} is positive (due to the domination of the kinetic energy contribution) and depends approximately linearly on z, $\widetilde{H}_{12}$ is negative and displays a minimum near z_0. The dramatic difference between H_{12} and $\widetilde{H}_{12}$ is a consequence of the -SH_{11} term in the numerator of eq 7. Obviously, the minimum in $\widetilde{H}_{12}$ translates to a maximum in ${\widetilde{H}_{12}}^2$.

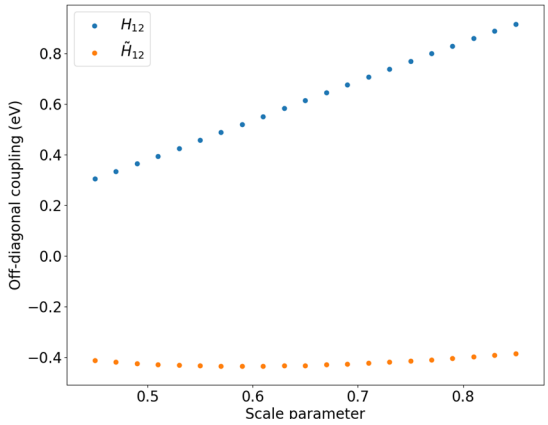

Figure 7. H_{12} and $\widetilde{H}_{12}$ vs. scale parameter for the two-level treatment of the D resonance of the finite spherical well problem.

Several "special" points, some of which have already been mentioned, can be associated with the two-state stabilization graph. These are summarized in Table 2. The most important is the stationary point, z*, which is associated with the complex resonance energy. Consistent with stabilization calculations on other models and on atoms and molecules this is located further in the complex plane than the branch point, z_b.[19] Other "special" points include, z_0, the crossing point of the diabatic curves, z_2 the point of closest approach of the adiabatic curves, and z_1, the point at which $\widetilde{H}_{12}$ has its minimum. z_0 and z_2 are close in value and are somewhat larger than z_1. Note, that if $\widetilde{H}_{12}$ were constant, then $z_0 = z_2$. The values of these special points are dependent on the basis set used for the stabilization calculation.

Table 2. Special points derived from the two basis function stabilization calculation described in the text.

Special point	z value
z_b (branch point)	0.723 – 0.306i
z^* (stationary point)	0.580 – 0.386i
z_0 ($H_{11} = \widetilde{H}_{22}$)	0.649
z_1 ($\widetilde{H}'_{12} = 0$)	0.590
z_2 (minimum of $E_+ - E_-$)	0.660

Although we have analytical expressions for H_{12} and S, and, thus, also for $\widetilde{H}_{12}$, for the two basis function stabilization calculation on the D resonance of the finite spherical well problem, the resulting expression for $\widetilde{H}_{12}$, particularly when using the contracted function with five primitive GTOs for the discrete state, is quite involved. Hence, for the purpose of elucidating the role of overlap in establishing the shape of the $\widetilde{H}_{12}$ curve in the vicinity of z_1, it is more instructive to fit S and H_{12} to polynomials in powers of $y = z - z_1$, keeping terms though second order in y:

$$S \approx s_0 + s_1 y + s_2 y^2 \qquad (13)$$

$$H_{12} \approx h_0 + h_1 y + h_2 y^2 \qquad (14)$$

Least squares fitting these expansions of S and H_{12} to the results for z values between 0.45 and 0.85, gives s_0, s_1, and s_2 = 0.4998, 0.7316, and -0.4483, respectively, and h_0, h_1, and h_2 = 0.555, 1.556, and -0.106, respectively for H_{12} in eV.

Keeping terms up to order y^2, we have

$$\widetilde{H}_{12} \approx -0.435 + 0.729 y^2 \qquad (15)$$

Squaring this result, again retaining terms only up through quadratic in y gives

$$\widetilde{H}_{12}^{\,2} \approx 0.190 - 0.637 y^2 \qquad (16)$$

Thus, we see that the $s_0 H_{11}$ contribution to $\widetilde{H}_{12}$ is responsible for the square of the latter quantity being negative near z_1, and also that the negative curvature in $\widetilde{H}_{12}^{\,2}$ is due to the product of the constant and quadratic terms in $\widetilde{H}_{12}$.

Model Hamiltonian Results. As seen from the results reported in Table 1, sufficiently flexible GPA fits to the stabilization graph allow accurately location of the stationary point and determination of the associated complex resonance energy. However, greater insight into the factors important for establishing the stationary point and the complex resonance energy can be achieved by applying simpler, physically motivated, models with fewer parameters than in the higher order GPAs needed to achieve convergence. With this in mind, we now turn to the five-parameter model introduced in Ref. 24. In this model, with energies in eV:

$$H_{11} = c_0 \tag{17}$$

$$\widetilde{H}_{22} = c_0 + c_1(z - z') \tag{18}$$

$$\widetilde{H}_{12}^{\,2} = A + B(z - z')^2 \tag{19}$$

where the various parameters are obtained from a least-squares fit of E_+ and E_- using data points in the vicinity of an avoided crossing. Note that z' determined in this manner can differ from z_1 defined above. A fit of the two energy eigenvalues for this model Hamiltonian to the data in the stabilization graph for z values between 0.45 and 0.85 gives c_0, c_1, z', A, and B = 1.888, 3.195, 0.6606, 0.187, and -0.675, respectively.

Figure 8 compares for the two basis function treatment of the spherical well problem the $\widetilde{H}_{12}{}^2$ curves obtained directly from the analytical matrix elements as well as the fit of the model described above to the stabilization graph reported in Figure 4. The maximum in the curve deduced from our model Hamiltonian is shifted to a somewhat larger z value than the exact curve, however, the peak maxima and curvatures are in good agreement. Referring back to the results in Table 2, we see that the exact $\widetilde{H}_{12}{}^2$ curve is peaked close to the real value of the stationary point while that from our model is peaked close to the crossing point of the diabatic curves.

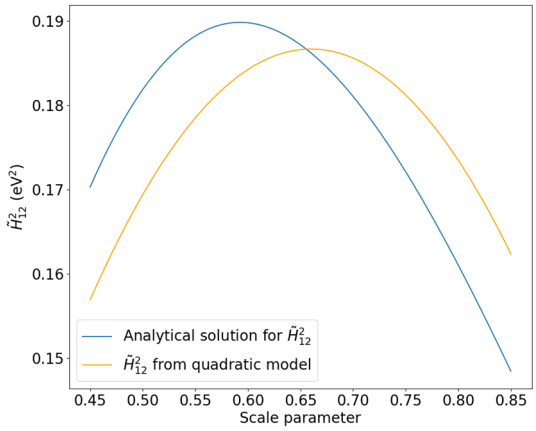

Figure 8. $\widetilde{H}_{12}{}^2$ *vs*. scale parameter for the two-level treatment of the *D* resonance of the finite spherical well problem. Both the exact result and that extracted from the stabilization graph using eqs 17-19 are reported.

While Figure 8 focuses on the range of z values from 0.45 to 0.85 we note that the exact $\widetilde{H}_{12}{}^2$ for the two basis function treatment is necessarily positive over the entire range of meaningful z-values (0 to about 2.0), whereas that given by eq 19 goes negative for z values less than about 0.1 and greater than about 1.2, which is unphysical, and is a consequence of the functional form adopted for $\widetilde{H}_{12}{}^2$. Interestingly, when scaling multiple basis functions and focusing on an avoided crossing flanked by other avoided crossing, $\widetilde{H}_{12}{}^2$ extracted from the stabilization graph (without any assumption concerning its functional form) also goes negative for small and large z values. In Ref. 24 it was postulated that this is a consequence of folding a multi-level problem into a two-level problem.

In reference 24, we showed that the relevant stationary point for this model Hamiltonian is given by

$$z^* = z' - \sqrt{\frac{c_1 A}{|B|(c_1^2 + 4B)}}\, i \qquad (20)$$

and that the associated complex resonance energy is

$$E_{res} = c_0 - 2i\left[\left(\frac{\sqrt{A|B|}}{\sqrt{4B + c_1^2}}\right)\right] \qquad (21)$$

The existence of the complex stationary point, and hence, the resonance, requires that the curvature B be negative. Although the parameters in this model were obtained by fitting the stabilization graph with the assumption that $\widetilde{H}_{22}$ is linear rather than using the fits to the exact matrix elements (eqs 13 – 15), it is still useful to analyze the coefficients A and B in eq 19 in terms of the earlier analysis involving the series expansions of H_{12} and S. In particular, we note that the A and B coefficients determined from fitting the model to the stabilization graph are close to coefficients of the constant and quadratic terms in eq 16. We further see that B is given by the product of the constant and quadratic terms in $\widetilde{H}_{12}$, and that it is negative due to the domination of the s_0h_{11} factor in the (h_0 - s_0h_{11}) contribution. Because z′ from the fit of the model to the stabilization graph differs slightly from z_1, the expression for $\widetilde{H}_{12}{}^2$ for the model contains a small linear term when expanded about z'. However. this term is very small and does not impact the above analysis.

In the limit that $c_1^2 >> 4B$ the half width reduces to $2\sqrt{A|B|}/c_1$. Using the parameters obtained by fitting the stabilization graph to the 2x2 model described by Equations 17 - 19, this approximation gives a half width of 0.222 eV, as compared to the 0.259 eV result from eq 21, and 0.278 eV from analytical expressions for the adiabatic energies.

We now briefly comment on the alternative two-level model for extracting resonance parameters from a stabilization graph introduced by Simons[22]. This model assumes that the two diabatic curves vary linearly with z near the avoided crossing and that the coupling is a constant. Fits of the Simons model or our model to the data from a stabilization graph result in the same values of the resonance energy and width. The connection between the two models can be seen by rewriting the quantity under the square root of eq 9 as $(H_{11} + H_{22})^2 + 4(H_{12}^2 - H_{11}H_{22})$. Here we have dropped the tildes since the terms impacted by orthogonalization differ in the two models. In both models $H_{11} + H_{22}$ depends linearly on z, a consequence of which is that $H_{12}^2 - H_{11}H_{22}$ must display at least a quadratic dependence on z for the existence of complex stationary points. In our model this dependence enters through H_{12}^2 whereas in the Simons model it enters through the $H_{11}H_{22}$ term. In fact, one can show that the two models are related as follows:

$$a_2 = 0.5[c_1 + \sqrt{c_1^2 + 4B}\,] \qquad (22)$$

$$a_1 = 0.5[c_1 - \sqrt{c_1^2 + 4B}\,] \qquad (23)$$

where a_1 is the slope of the discrete state and a_2 the slope of the DC level in the Simons model. As noted above, B is negative and c_1^2 is appreciably larger in magnitude than $4B$. Hence the slope of H_{11} in Simons model is a consequence of the overlap between ψ_1 and ψ_2. Importantly, the conclusion of the vital role of overlap in establishing the resonance properties is independent of which of these models one adopts. We further note that, the 012 GPA in which $H_{11} + H_{22}$ also has a linear z dependence and $H_{12}^2 - H_{11}H_{22}$ includes terms up through quadratic in z, gives resonance parameters identical to those from our model and the Simons model. However, the 012 GPA, unlike these two models, does not allow determining whether the quadratic dependence on the scale parameter is split across the H_{12}^2 or $H_{11}H_{22}$ terms.

CONCLUSIONS

In this study we have presented the results of a minimalist two-level stabilization calculation of a *D* resonance of a simple model potential. Although such a treatment is not expected to give quantitatively accurate resonance parameters, it has the advantage of making clearer the role of the overlap between the discrete state and a DC level in establishing resonance parameters, and it provides a test for assessing the convergence of GPAs for extracting the resonance energy. With the assumption that the energy of the discrete state, H_{11}, is independent of the scale parameter z, we show that for this model, the square of the off-diagonal coupling, $\widetilde{H}_{12}{}^2$, is peaked near the crossing point of the diabatic curves, just as we found previously for stabilization calculations on the Π_g anion of N_2. We further show that this is a consequence of the overlap contribution that arises from the orthogonalization of the wave function associated with the DC level to that of the discrete state. We also apply the model Hamiltonian that we introduced in Ref. 24 to this problem, showing that with the additional assumption that $\widetilde{H}_{22}$ varies linearly with z, the negative curvature in $\widetilde{H}_{12}{}^2$ is essential for the existence of the resonance for the finite spherical well problem. We also examine more closely the connection of our model Hamiltonian approach and that of Simons which assumes that the off-diagonal coupling is independent of z and that both H_{11} and H_{22} are linear in z. The two models give identical resonance parameters, but the effect of orthogonalization is manifested differently in the diagonal and off-diagonal matrix elements. We also obtain resonance parameters for the two-level stabilization calculations directly from the analytical expression for the energy levels and show that it is necessary to use a GPA with as many as 14 parameters to obtain results in close agreement with that obtained without fitting.

ASSOCIATED CONTENT

Supporting Information

The Supporting Information is available free of charge at https://pubs.acs.org

Analytical expressions for the overlap, kinetic energy and potential energy integrals evaluated using Gaussian-type orbitals. Also, the contraction coefficients for the wave function for the discrete state.

ACKNOWLEDGEMENTS

SS and KDJ acknowledge the support of the National Science Foundation under grant CHE1762337 and MFF acknowledges support from the Swezey research fund at Grove City College.

REFERENCES

1. Schulz, G. Resonances in Electron Impact on Diatomic Molecules. *Rev. Mod. Phys.* **1973**, *45*, 4234–86.

2. Jordan, K. D.; Burrow, P. D. Temporary Anion States of Polyatomic Hydrocarbons, *Chem. Rev.* **1987**, *87*, 5575–88.

3. Jordan, K D.; Burrow, P. D. Studies of the Temporary Anion States of Unsaturated Hydrocarbons by Electron Transmission Spectroscopy, *Acc. Chem. Res.* **1978**, *11*, 341–348.

4. Campbell, L.; Allan, M.; Brunger, M. J. Electron Impact Vibrational Excitation of Carbon Monoxide in the Upper Atmospheres of Mars and Venus. *J. Geophys. Res.* **2011**, *116*, A09321.

5. Larsson, M. Imitating Electron-Molecular Ion Collisions in Interstellar Space at Extremely Low Temperatures Using a Storage Ring. *Phys. Scr.* **1995**, *T59*, 270–277.

6. Gorse, C.; Cacciatore, M.; Capitelli, Kinetic Processes in Non-Equilibrium Carbon Monoxide Discharges. I. Vibrational Kinetics and Dissociation Rates. M. *Chem. Phys.* **1984**, *85*, 165–176.

7. Alizadeh E.; Sanche, L. Measurements of *G* Values for DNA Damage Induced by Low-Energy Electrons. *J. Phys. Chem. B*. **2011**, *115*, 14852–14858.

8. Balslev E.; Combes J. M. Spectral Properties of Many-body Schrödinger Operators with Dilatation-analytic Interactions. *Commun. Math. Phys.* **1971**, *22***,** 280–294.

9. Riss, U. V.; Meyer, H.-D. Calculation of Resonance Energies and Widths Using the Complex Absorbing Potential Method. *J. Phys. B* **1993**, *26*, 45034–535.

10. Horáček*,* J.*;* Paidarová*,* I.; Čurík, R. On a simple way to calculate electronic resonances for polyatomic molecules. *J. Chem. Phys.* **2015**, *143*, 184102.

11. Hazi, A. U.; Taylor, H. S. Stabilization Method of Calculating Resonance Energies: Model Problem. *Phys. Rev. A* **1970**, *1*, 1109–1120.

12. Siegert, A. J. On the Derivation of the Dispersion Formula for Nuclear Reactions. *Phys. Rev*. **1939**, *56*, 750–752.

13. Dube, L.; Herzenberg, Absolute Cross Sections from the Boomerang Model for Resonant Electron-Molecule Scattering, A. *Phys. Rev. A* **1979**, *20*, 194–213.

14. Chao, J. S. Y.; Falcetta M. F.; Jordan, K. D. Application of the Stabilization Method to the $N_2^-(X^2\Pi_g)$ and $Mg^-(1^2P)$ Temporary Anion States. *J. Chem. Phys.* **1990**, *93*, 1125–1135.

15. Falcetta, M. F.; DiFalco, L. A.; Ackerman, D. S.; Barlow, J. C.; Jordan, K. D. Assessment of various Electronic Structure Methods for Characterizing Temporary Anion States: Application to the Ground State Anions of N_2, C_2H_2, C_2H_4 and C_6H_6, *J. Phys. Chem. A* **2014**, *118*, 7489–7497.

16. Jagau, T.-C.; Bravaya, K. B.; Krylov, A. I. Extending Quantum Chemistry of Bound States to Electronic Resonances. *Annual Rev. of Phys. Chem*. **2017**, *68*, 525–553.

17. Møller, C.; Plesset, M, S. Note on an Approximation Treatment for Many-Electron Systems. *Phys. Rev.* **1934**, *46,* 618–622.

18. Stanton, J. F.; Gauss, J. Perturbative Treatment of the Similarity Transformed Hamiltonian in Equation-of-Motion Coupled-Cluster Approximations. *J. Chem. Phys.* **1995**, *103*, 1064–1076.

19. McCurdy, C. W.; McNutt, J. F. On the Possibility of Analytically Continuing Stabilization Graphs to Determine Resonance Positions and Widths Accurately. *Chem. Phys. Lett.* **1983**, *94*, 306–310.

20. Isaacson A. D.; Truhlar, D. G. Single-root, Real-basis-function Method with Correct Branch-point Structure for Complex Resonances Energies. *Chem. Phys. Lett.* **1984**, *110,* 130–134.

21. Mandelshtam, V. A.; Ravuri, T. R.; Taylor, H. S. Calculation of the Density of Resonance States Using the Stabilization Method. *Phys. Rev. Lett.* **1993**, *70*, 1932–1935.

22. Simons, J. Resonance State Lifetimes from Stabilization Graphs. *J. Chem. Phys.* **1981**, *75*, 2465–2467.

23. Jordan, K. D. Construction of Potential Energy Curves in Avoided Crossing Situations. *Chem. Phys.* **1975**, *9*, 199–204.

24. Carlson, B. J.; Falcetta, M.F.; Slimak, S. R.; Jordan, K. D. A Fresh Look at the Role of the Coupling of a Discrete State with a Pseudocontinuum State in the Stabilization Method for Characterizing Metastable States, *J. Phys. Chem. Lett.* **2021**, *12*, 1202–1206.

25. Wheeler, J. A. On the Mathematical Description of Light Nuclei by the Method of Resonating Group Structure, *Phys. Rev.* **1937**, *52*, 1107–1122.

26. Johnston, A. R.; Gallup, G. A.; Burrow, P. D. Low-lying negative-ion states of calcium, *Phys. Rev. A*. **1989**, *40*, 4770–4773.

27. Landau, A.; I. Haritan, The Clusterization Technique: A Systematic Search for the Resonance Energies Obtained via Padé. *J. Phys. Chem. A* **2019** *123*, 5091–5105.

TOC Graphic

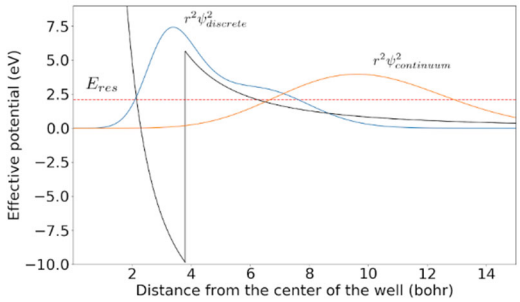
$r^2\psi^2_{discrete}$
$r^2\psi^2_{continuum}$
E_{res}
Effective potential (eV)
7.5
5.0
2.5
0.0
−2.5
−5.0
−7.5
−10.0
2
4
6
8
10
12
14
Distance from the center of the well (bohr)